JOURNAL OF SOLID STATE CHEMISTRY 77, 72–83 (1988)

The Incorporation of Selenium into the Channels of Mordenite: An Electron Microscopic Study

O. TERASAKI,* K. YAMAZAKI,* J. M. THOMAS,† T. OHSUNA,‡ D. WATANABE,* J. V. SANDERS,§,‖ AND J. C. BARRY¶

Department of Physics, Tohoku University, Sendai 980, Japan; †Davy Faraday Research Laboratory, The Royal Institution, 21 Albemarle Street, London W1X 4BS, United Kingdom; ‡JEOL, EOD EMG, Akishima 196, Japan; §Division of Materials Science, CSIRO, Normanby Road, Clayton, Victoria 3168, Australia; and ¶Centre for Solid State Science, Arizona State University, Tempe, Arizona 85287

Received April 25, 1988

Mordenite (idealized formula $Na_8Al_8Si_{40}O_{96} \cdot 24H_2O$), a zeolite which has one-dimensional channels (diameter ca. 7 Å) running parallel to its *c*-axis, is shown to be capable of assimilating chains of selenium when the latter is introduced from the vapor phase. As the centers of the main channels in mordenite are separated by ca. 13.5 Å, this is a novel method of producing low-dimensional solids. The resulting material has been characterized by high-voltage–high-resolution electron microscopy (1 MeV) and image calculations. No selenium is taken up in the subsidiary channel system of mordenite, and there is a strong tendency for "patchwise" uptake, some channels being free and others full of selenium.

Introduction

Zeolites are a class of aluminosilicates with open structures in which the channels and cages are of dimensions comparable with those of the cross sections of small inorganic (H_2O, H_2S, SO_2, NH_3, Hg . . .) or small organic (C_1 to C_8 straight-chain and methyl-substituted straight-chain hydrocarbons) molecules; see literature (*1–3*) for further details. The role of zeolites as adsorbents and catalysts has been well documented (*4–6*); but only very recently has it been realized that they are potentially very valuable hosts for the accommodation of condensed matter under conditions of restricted geometry (*7, 8*).

Certain zeolites possess one-dimensional channels, others a system of two perpendicular or inclined but nonintersecting one-dimensional channels, while yet others have intersecting channels. The scope for designing novel low-dimensional solids, in which the degree of interaction between contiguous chains of guest species may be controlled, is, therefore, quite considerable. We discussed such possibilities in an earlier preliminary publication (*9*). Other workers have described the interesting electrical and optical properties displayed

‖ Deceased, December 1987.

0022-4596/88 $3.00

by the chalcogens, selenium and tellurium, when assimilated by zeolitic hosts (*10*).

It has been confirmed that high-resolution electron microscopic images of zeolites provide direct information about framework structures and various kinds of defects (*11–13*). The technique of electron microscopy (*14*) can therefore be used to detect any faults resulting from the insertion of Se and, further, to identify the relative positions between the framework of the zeolite and the Se chain.

Structural Background

The crystal structure of mordenite (*15*) is presented in Fig. 1. It has a space group *Cmcm* with unit-cell parameters of $a = 18.1$ Å, $b = 20.5$ Å, $c = 7.5$ Å, and it consists of large apertures made up of 12 corner-linked tetrahedra (TO_4; $T = Si^{4+}$ or Al^{3+}). The stacking is such that there is a main channel system running perpendicular to the plane of the 12-membered rings and parallel to the *c*-axis. The projected potential density along this axis is also shown in Fig. 1.

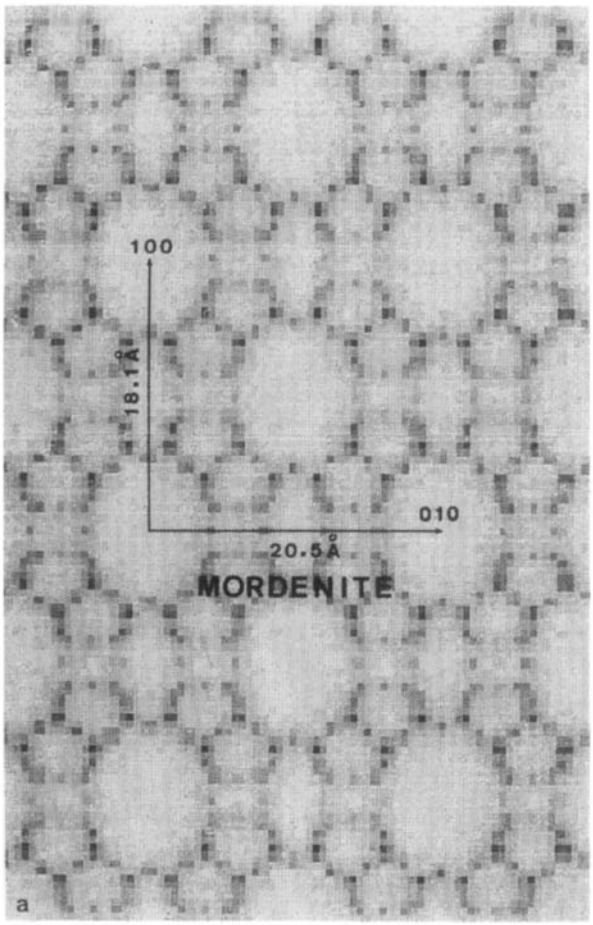

FIG. 1. (a) Projected potential density (along [001]) of mordenite, and (b) schematic drawing of its framework structure. The structure of crystalline Se is shown, in elevation, in (c), and a projection of the chain of Se along the *c*-axis is shown in (d). Note that, from the scale of these drawings, only one chain of Se can be accommodated in the main channels of mordenite.

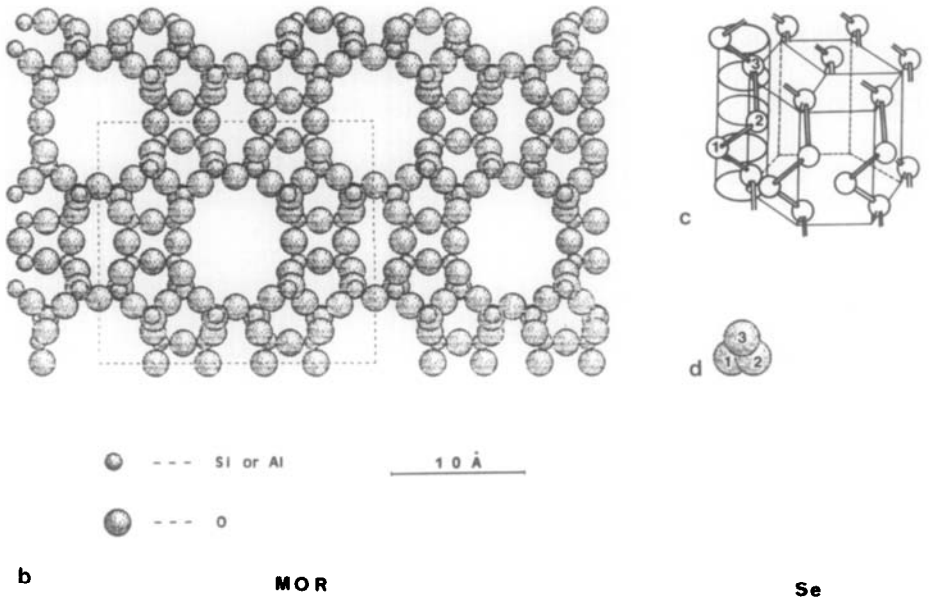

Crystalline selenium has the so-called A8 structure composed of parallel spiral chains (Fig. 1c): the intrachain bonds are covalent, whereas interchain ones are of van der Waals character.

Agroskin *et al.* (*16*) and Bogomolov *et al.* (*17*) reported upon the absorption spectra of chains of selenium housed within the channels of a single crystal of natural mordenite and observed strong anisotropy. Tamura *et al.* (*18*), using extended X-ray absorption fine-structure to probe mordenite which had assimilated some selenium, reported that the intrachain separation distance of the Se atoms was marginally reduced by comparison with that of the pure crystalline guest.

From the projected drawing of the selenium spiral it follows that double occupancy of the main channels is unlikely and even single occupancy of the subsidiary channels is forbidden.

Hitherto there has been no direct study of the structural details of incorporation of selenium into zeolites. We have shown that a variety of zeolites may be used as hosts (ZSM-23, ZSM-5, and zeolites L and Y). Here we concentrate on the mordenite–selenium system and, in particular, verify that the chains of guests do indeed run along the axis of the main channels, and that there is an unexpected "patchiness" (domain character) to the uptake in the sense that not all channels of the mordenite are occupied by selenium.

Experimental

Samples of synthetic mordenite in the H^+-exchanged form were provided by the Catalysis Society of Japan (JRC-Z-HM20). The Si/Al ratio was nominally 10. Prior to exposure to selenium, the zeolite samples were dehydrated gently by heating up to 350°C and kept for 5 hr under vacuum (better than 1.0×10^{-5} Torr). They were sealed in a Pyrex glass tube with elemental selenium (99.999 purity) and then heated at 400°C for 3 hr prior to being cooled slowly to room temperature. The mordenite

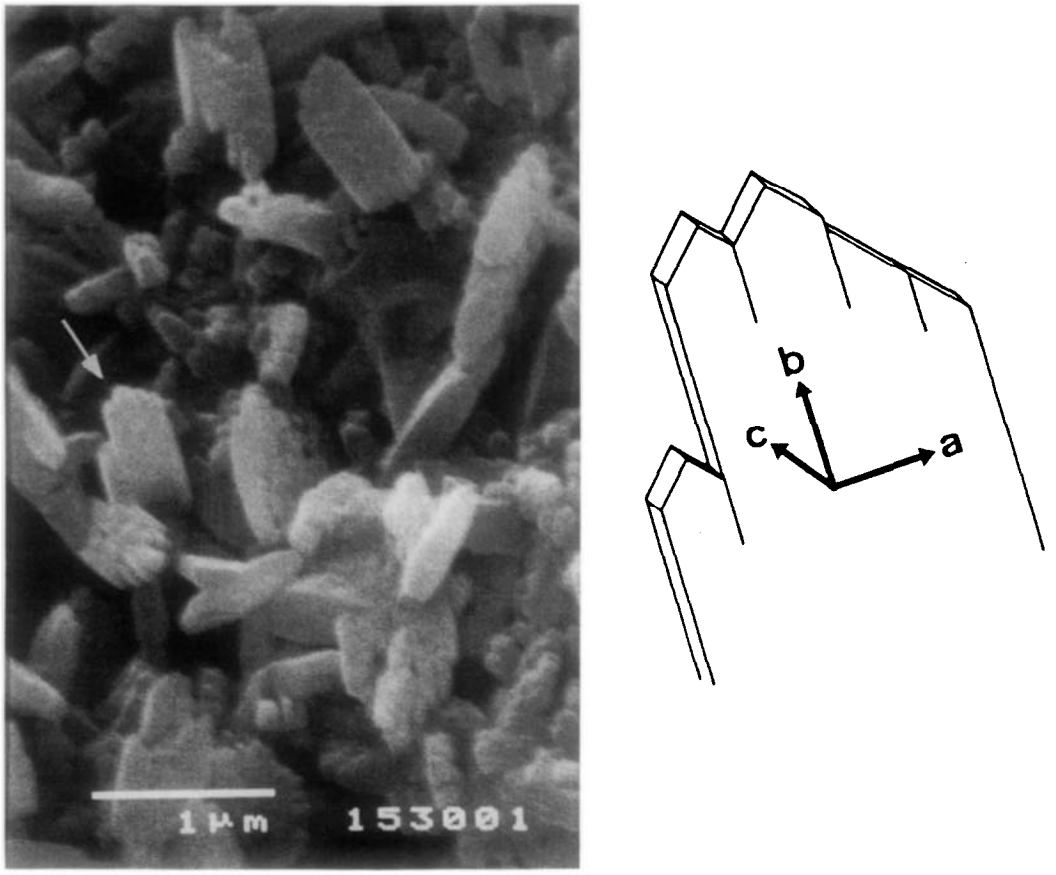

FIG. 2. A scanning electron micrograph of mordenite (a), and a schematic drawing showing the relationship between crystal shape and axes (b).

changed from white to an orange color upon incorporation of the selenium.

Specimens of the product were crushed in an agate mortar under acetone, collected in a microgrid, and examined in a JEM-1000 high-resolution electron microscope fitted with a top-entry goniometer. The selenium content was determined from the X-ray emission spectra generated by electron irradiation in a scanning electron microscope (JSM-T330).

A scanning electron micrograph, along with a sketch showing the morphology and its crystallographic identity, is shown in Fig. 2. The crystals have a plate-like character, being somewhat elongated along the *b*-axis and thin along the *c*-axis. Since the Al K-emission X-ray peaks overlap the Se L-peaks, the contribution of the latter was separated from the former by estimating it from Se–K peaks. The elemental ratio turned out, globally, to be Al : Si : Se = 5 : 27 : 5. The ratio of the selenium to that of the total tetrahedral content (*T* atoms) is therefore 0.15, and it is to be noted that the average Si/Al ratio is 5.4.

Results and Discussion

First we describe the image simulations, then the principal features of the high-resolution micrographs.

(a) Image Simulations

These computations were performed on the basis of the following operating conditions: accelerating voltage, 1 MeV; spherical aberration coefficient of the objective lens, Cs, 11 mm; beam divergence, 0.5 Mrad; spread of focus, 260 Å; and resolution, 1.9 Å. The atomic coordinates of the framework atoms in the mordenite were taken to be the same as those given by Meier (*15*), prior to and after uptake of selenium—the error involved is known (*19*) to be negligible for present purposes. It was further assumed that the chains of selenium in the mordenite take up the same atomic positions as those of the corresponding chains in the crystalline solid (Fig. 1c) so that the scattering amplitudes for *hk*0 reflections were calculated from the projected arrangement (Fig. 1d) by taking account of the probability of occupation. Finally, it was assumed that there is only one chain situated centrally in each of the main channels.

Computed, through-focus, through-thickness series of images are shown in Figs. 3a and 3b for the mordenite with and without selenium, respectively. From these series we see that, provided the specimen thickness is less than 150 Å and that the extent of defocus falls between −750 and −1150 Å (i.e., around the Scherzer focus), both the main and subsidiary channels of the zeolite are imaged as white dots (of larger or smaller size, respectively) for the pure mordenite. When the selenium is present the contrast of the main channels changes to dark dots, whereas that of the subsidiary channels remains white.

(b) High-Resolution Images

Figure 4 shows the high-resolution image along [001] and the corresponding electron diffraction pattern of mordenite without incorporated selenium. The presence of the subsidiary and main channel systems is clearly seen in this projected image. There is a significant change in the image contrast under comparable conditions when selenium is present (Fig. 5). Black and white contrast dominates the image, and the wavy, dark bands are roughly perpendicular to the [010] direction with a period of ca. 100 Å. The area of black contrast amounts to some 70% of the total area of the image. Such black–white contrast is never observed for the mordenite devoid of selenium: it is indisputably a consequence of the incorporation of the chalcogen. But is the selenium inside or lodged on the exterior surface of the host? Electron diffraction patterns (typified by Fig. 6) show some diffuse spots indicative of the modulation of the parent structure, but there are no sharp reflections or diffuse rings from segregated selenium.

The higher magnification image shown in Fig. 7 further clarifies the contrast between the black and the white regions of Fig. 5. It is to be noted that the image of the "white" regions is almost indistinguishable from that of the parent mordenite: the main and subsidiary channel systems are both imaged as white dots. In the black bands of Figs. 5 and 7, the contrast of the main channels is dark whereas that of the subsidiary channels remains white. This fact, along with the simulated images described above, signifies that the selenium is indeed sorbed in the main channels of the mordenite.

If we assume that the interatomic distances of the selenium in the free and sorbed state are the same—and the results of Tamura *et al.* (*18*) justify this assumption—we compute the ratio of the total possible number of Se atoms to that of the tetrahedral (*T*) atoms in mordenite to be 0.19. The experimental Se/*T* ratio, as stated earlier, is 0.15, and the ratio of these two values, 0.8, is quite close to the ratio of the area of black regions to the total area of the high-resolution micrograph. This is in line with the interpretation that the selenium is

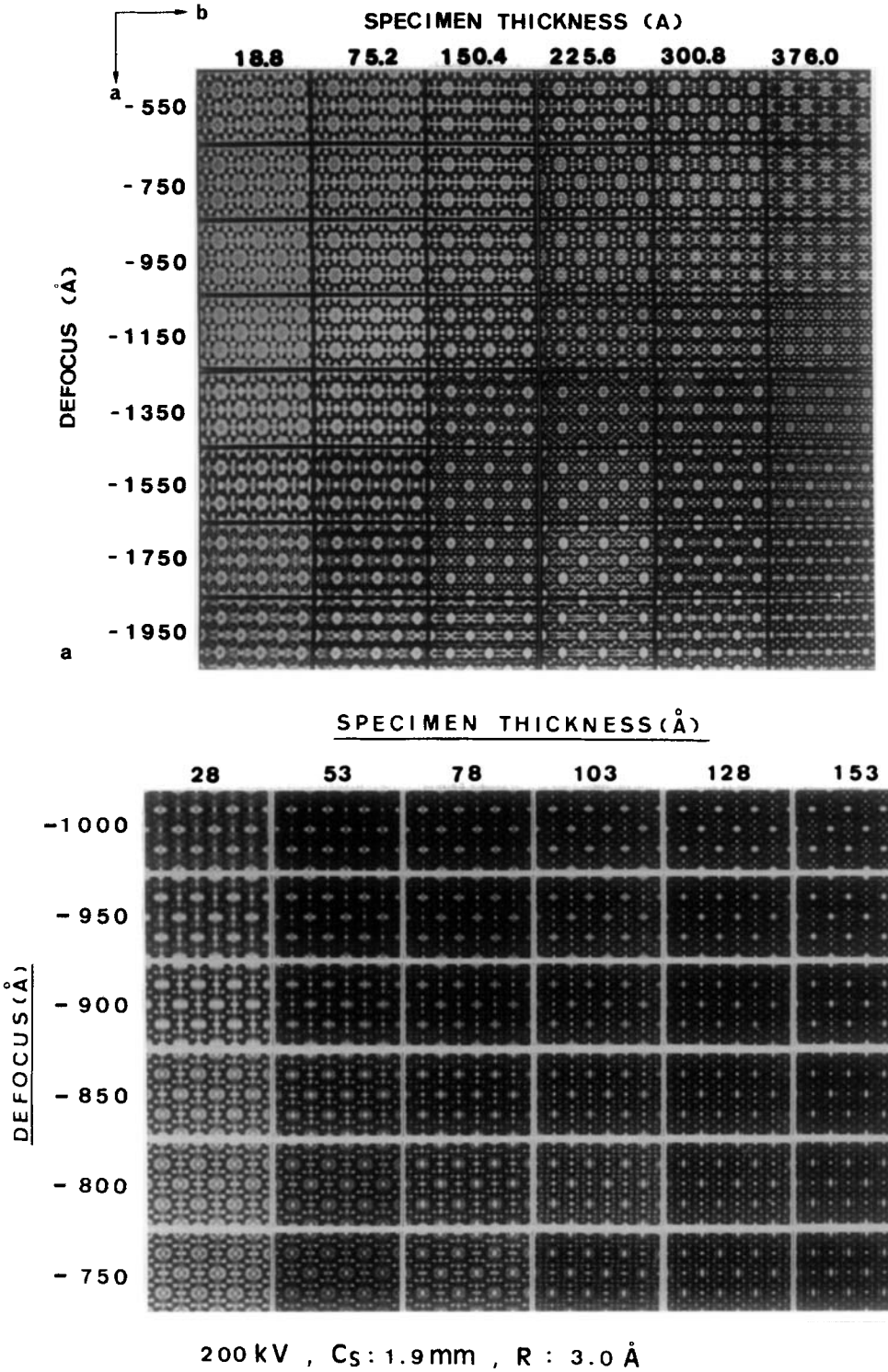

FIG. 3. Computed images of mordenite without (a) and with (b) Se in the major channels. (Viewed down [001] in each case—see text for conditions of imaging.)

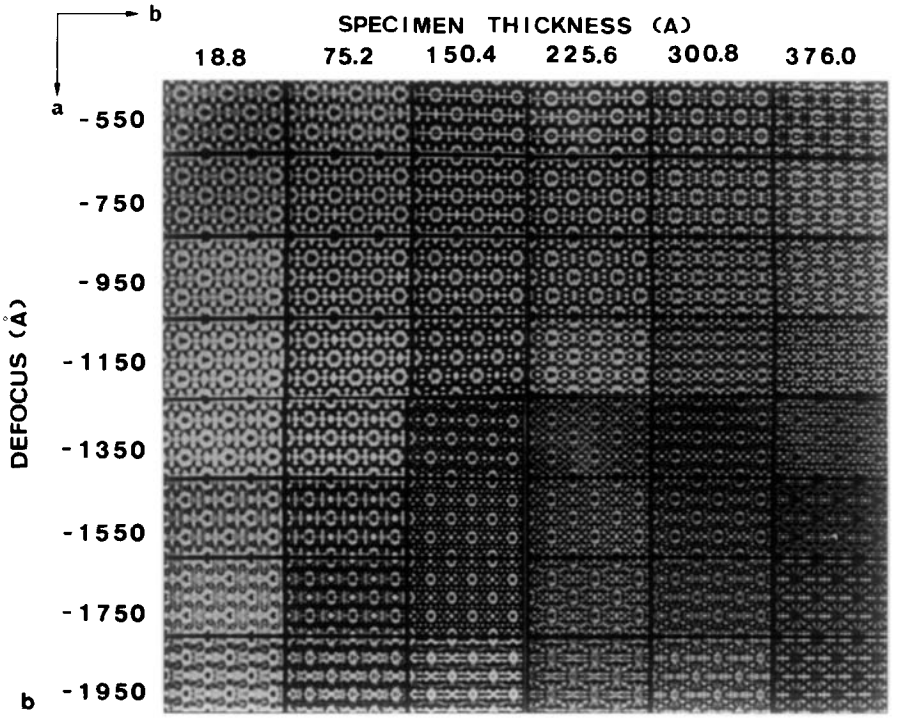

FIGURE 3—*Continued.*

incorporated as chains into the main channels. Clearly (from Figs. 5 to 7) the framework structure of the mordenite host remains intact. Interestingly, the lifetime of the host–guest complexes in the electron beam significantly surpasses that of the free host.

Preliminary work indicates that dark–white modulation is observed only in mordenite as host for selenium. For other zeolites a different Se/*T* ratio is obtained. The period of the modulation seems to be independent of—but the degree of contrast, as well as the width of the black bands, is dependent on—the concentration of the chalcogen. We therefore conclude that the main source of the black–white region in the high-resolution micrographs is amplitude contrast, because the band contrast does not change when the value of defocus changes from over to under focus.

With excess selenium used in the preparation of the mordenite complex, the black and white wavy contrast was still obtained. If no change such as elastic strain is introduced in the framework structure by Se, all channels should be filled. But, using optical diffractometry (*20*) on the dark and white regions of the image (Fig. 7), no discernible differences in lattice spacings were found as between the two regions. This is consistent with our X-ray diffractometry (not shown), from which we see no appreciable broadening in reflection profiles after treatment of the mordenite with selenium. Very small expansion of unit-cell dimensions was, however, detected.

We are not, however, in a position to be definitive about the root cause of the patchwise or domain character of the uptake of selenium by the mordenite. One possibility is that the dark–white regions

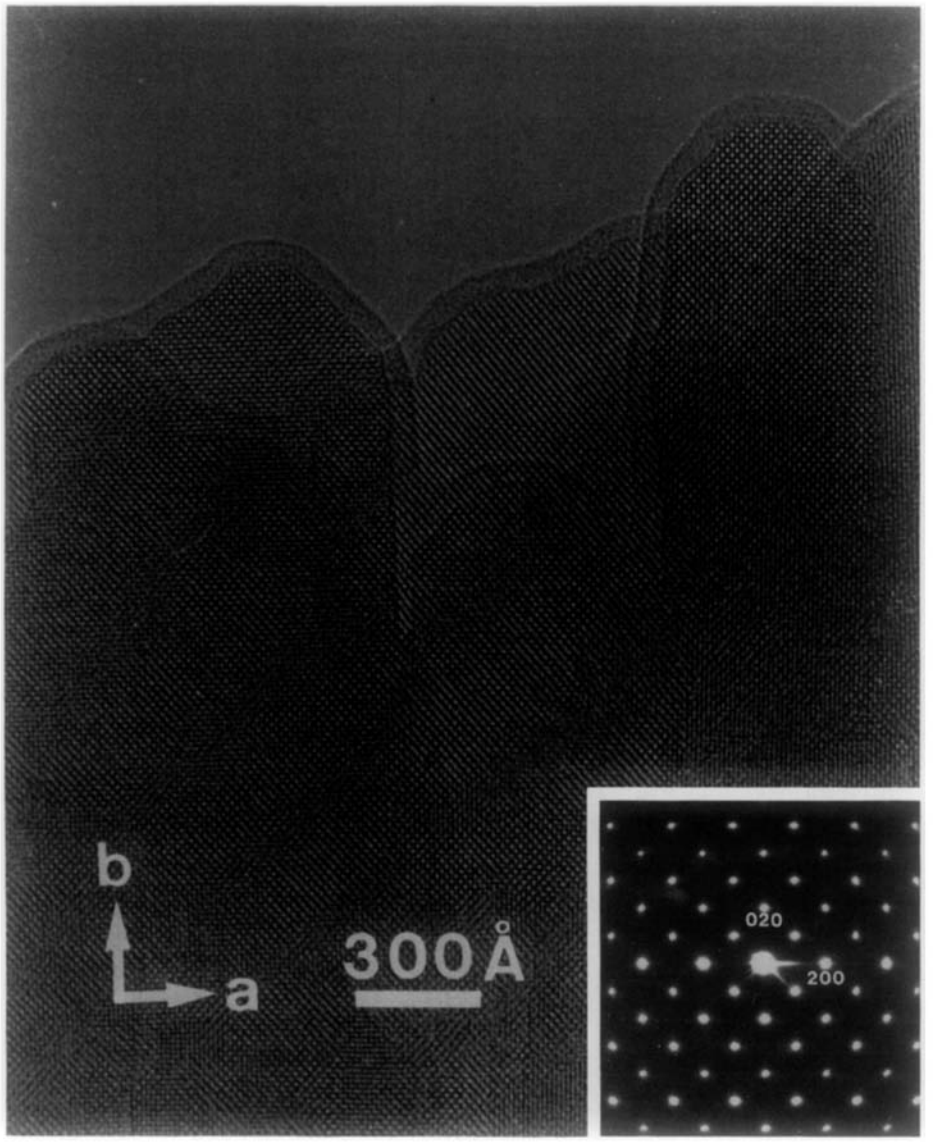

FIG. 4. A high-resolution electron micrograph of mordenite without Se viewed along [001]. Inset shows corresponding electron diffraction pattern.

arise, indirectly, from local differences in the Si/Al ratio. An Al-rich region could have somewhat constrained pores, and, in any case, would have more exchangeable cations (H^+) housed in the main channels. This is not likely, but until ultra-precise, spatially-localized X-ray emission studies are carried out it cannot be eliminated as a possible cause. Another possibility is that we could be seeing here a direct conse-

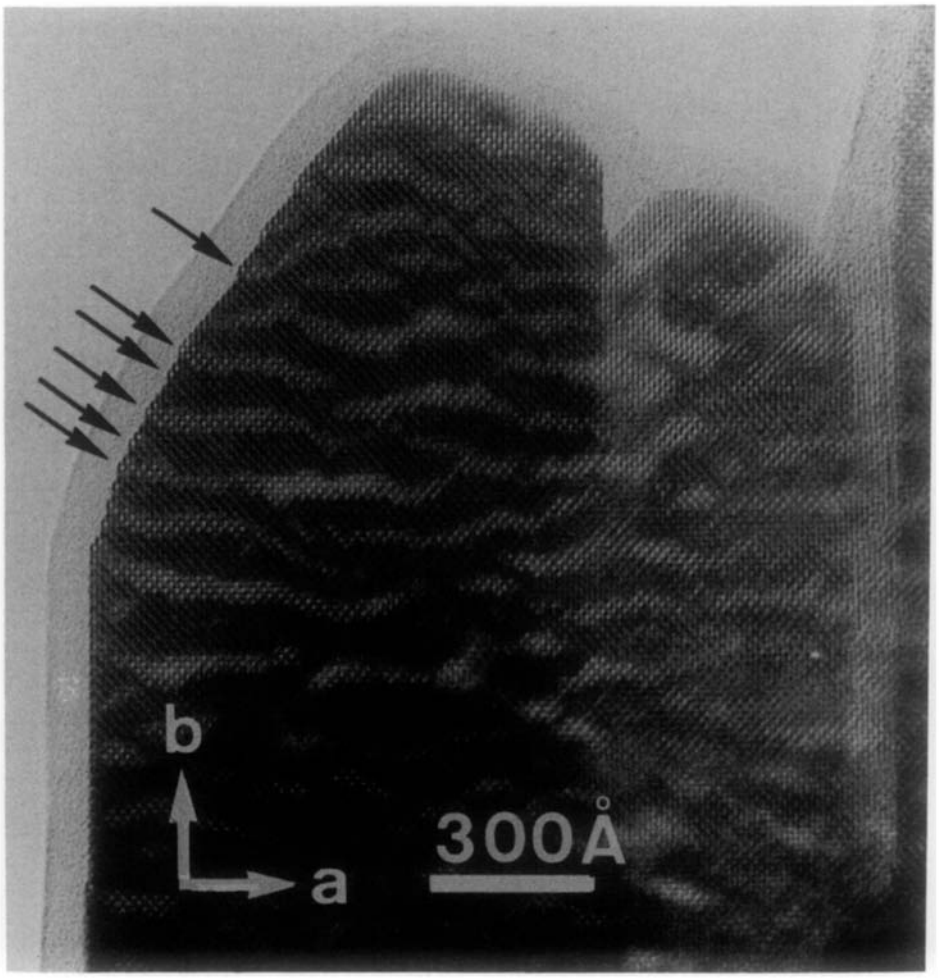

FIG. 5. High-resolution image of mordenite with Se in some of the main channels. Note the subunit-cell steps clearly visible at the periphery (see text).

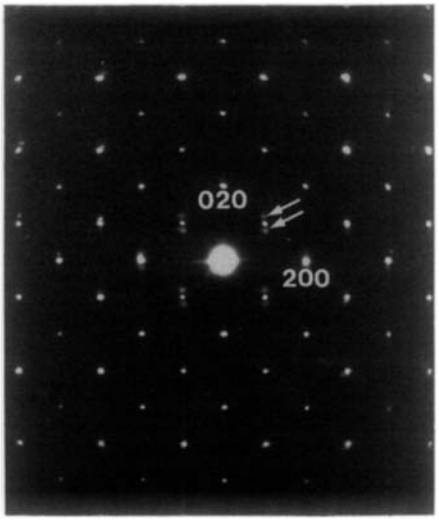

FIG. 6. The electron diffraction pattern ([001] zone axis) of a mordenite crystal containing Se. Note the diffuse features around the sharp spots from the parent mordenite.

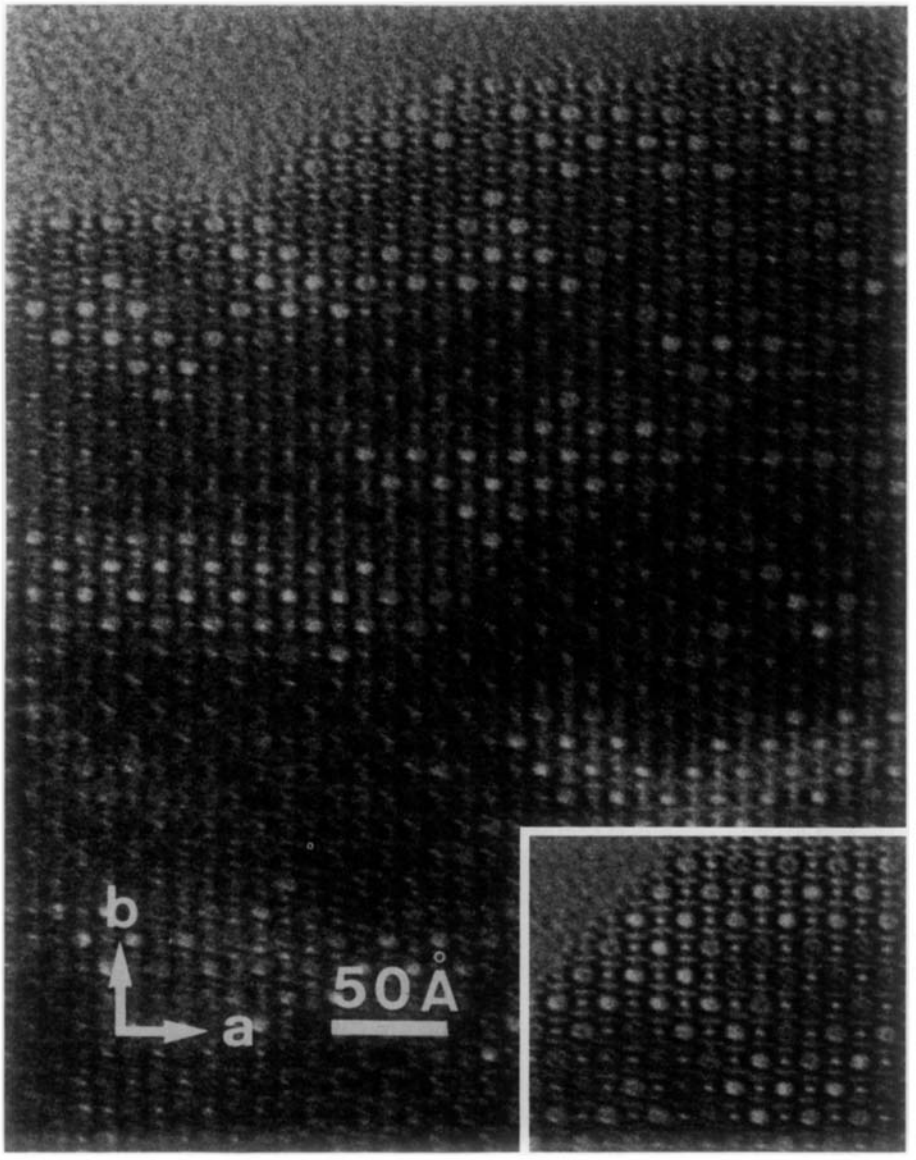

FIG. 7. High-resolution micrograph of mordenite containing assimilated Se. The large white dots, visible more clearly in the inset, are the main channels in the projection. The shortest distance separating these main-channel openings is ca. 13.5 Å. Dark contrast signifies a region where Se is present as guest.

quence of the renowned tendency for mordenite to exhibit narrow-pore or wide-pore behavior. The implication is that if the mordenite contains coexistent wide- and narrow-pore regions, selenium would be able to enter the former but not the latter. A

third, but less likely possibility is that the dark–white regions are a consequence of spinodal decomposition.

If Se enters into the main channels directly from the vapor and there is no structure modulation in mordenite there would be no reason for the contrast to appear in two different ways. What is the origin of the differentiation of the regions? As can be seen in Fig. 5, all the stepped edges (indicated by arrows in the figure) demarcate the places where the dark regions terminate. This strongly suggests that there is a correlation between surface steps or crystal morphology and the regions where a Se-string can exist in the crystal. Three possible explanations may be formulated.

(i) There is little doubt about the existence of two types of mordenite (vide the so called wide-pore and narrow-pore varieties) with different aperture sizes, mentioned above. Although the precise origin of this difference is not known (*2*), the aperture size of the narrow-pore variety is thought to be smaller than 4 Å in diameter, and there is consequently little chance of introducing Se into the channels. Summarizing, it may be that the black and white bands correspond to wide-pore and narrow-pore regions, respectively.

(ii) From the shape of mordenite crystals seen by scanning electron microscopy, there is obviously anisotropy in the rate of crystal growth. If this growth rate depends upon the concentration of Al, then a density modulation of Al and, therefore, of exchangeable cations along the *b*-axis may occur. Two cases must be considered: (a) Se chains can enter into only some regions: (b) Se can enter everywhere at high temperature in the first place, but only in some regions can the Se chains remain in the channels during subsequent processes. Exchangeable cations could block the introduction of the Se chains into the channels in case (a) and prevent subsequent escaping from the channels in case (b). In this way we may envisage a density modulation of cations which gives rise to a modulation of incorporated Se.

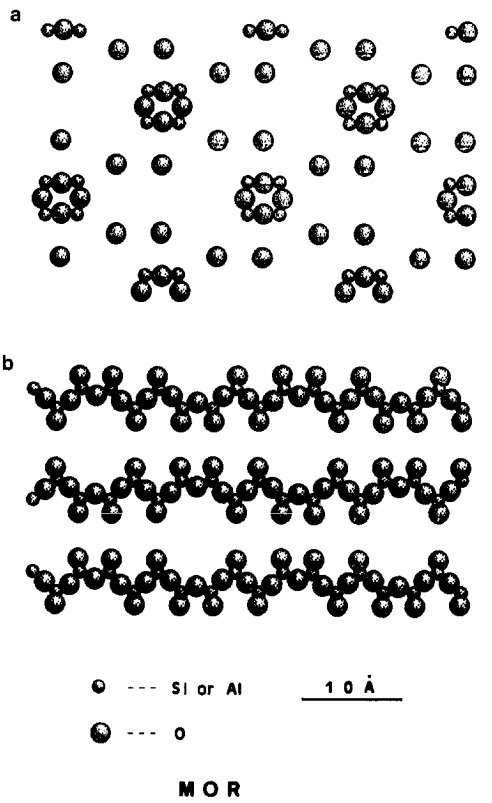

FIG. 8. Schematic drawings of two different atomic sheets (a and b) of the mordenite structure when cut conceptually parallel to the (001) plane.

(iii) Intermediate processes, implicating the crystal surface, need to be considered. If there are intermediate stages in the insertion, entailing local adsorption and surface migration of the bound selenium, we need to consider the details of the surface topography of the host. Mordenite can be divided conceptually into four sheets of thickness $c/4$ parallel to [001]. Two types of sheets with different atomic arrangements (Fig. 8) exist at $z = 0, 1/2$, and $z = 1/4, 3/4$. As the number of dangling bonds at these two types of exposed surface is the same, they will occur with the same frequency. But it

does not follow that the sticking coefficients and/or surface mobility (both being implicated in the process of incorporation) are the same. This could therefore govern the uptake of the selenium. Clearly more work, now underway, needs to be done to resolve these and related issues.

Acknowledgments

The authors thank Mr. H. Ota and Mr. E. Aoyagi for their help in the experiment. O.T. thanks Professor S. Andersson and Dr. Zoltan Blum (University of Lund) for suggesting the possibility of Al concentration modulation occurring during the crystal growth of mordenite. Part of this work was supported by a grant-in-aid from the Japanese Ministry of Education and by a British Council Academic Travel Grant (to O.T.). Further support from the Japanese Securities Scholarship Foundation (to O.T.) and the SERC (to J.M.T.) is gratefully acknowledged.

References

1. D. W. Breck, "Zeolite Molecular Sieves," Wiley, New York (1974).
2. R. M. Barrer, "Zeolites and Clay Minerals," Academic Press, New York/London (1978).
3. R. M. Barrer, "Hydrothermal Chemistry of Zeolites," Academic Press, New York/London (1982).
4. J. A. Rabo, *Catal. Rev. Sci. Eng.* **23,** 393 (1981).
5. J. M. Thomas, G. R. Millward, and L. A. Bursill, *Philos. Trans. R. Soc. A* **300,** 43 (1981).
6. J. M. Thomas, *J. Mol. Catal.* **27,** 59 (1983).
7. V. N. Bogomolov, *Sov. Phys. Usp.* **21**(1), 77 (1978).
8. K. Amaya and T. Haseda, *Butsuri* **39,** 793 (1984). [In Japanese]
9. O. Terasaki, K. Yamazaki, J. M. Thomas, T. Ohsuna, D. Watanabe, J. V. Sanders, and J. C. Bary, *Nature (London)* **330,** 58 (1987).
10. V. N. Bogomolov, V. V. Poborchy, S. G. Romanov, and S. I. Shagin, *J. Phys. C: Solid State Phys.* **18,** L313 (1985).
11. O. Terasaki, J. M. Thomas, and G. R. Millward, *Proc. R. Soc. London Ser. A* **395,** 153 (1984).
12. J. V. Sanders, *Zeolites* **5,** 81 (1985).
13. G. R. Millward, J. M. Thomas, O. Terasaki, and D. Watanabe, *Zeolites* **6,** 91 (1986).
14. J. M. Thomas, *Ultramicroscopy* **8,** 13 (1982).
15. M. W. Meier, *Z. Kristallogr.* **115,** 439 (1961).
16. L. S. Agroskin, V. N. Bogomolov, A. I. Gutman, A. I. Zadorozhnii, L. P. Rautian, and S. G. Romanov, *JEPT Lett.* **31,** 583 (1981).
17. V. N. Bogomolov, S. V. Khodlodkevich, S. G. Romanov, and L. S. Agroskin, *Solid State Commun.* **47,** 181 (1983).
18. K. Tamura, S. Hosokawa, H. Endo, S. Yamasaki, and H. Oyanagi, *J. Phys. Soc. Japan* **55,** 528 (1986).
19. J. M. Thomas and J. Klinowski, *Adv. Catal.* **33,** 199 (1985).
20. G. R. Millward and J. M. Thomas, *in* "Proceedings of the 4th London International Carbon and Graphite Conference 1974, London," Soc. Chem. Ind., London (1974).